

NEUTRONIC ANALYSIS STUDIES OF THE SPALLATION TARGET WINDOW FOR A GAS COOLED ADS CONCEPT.

**A. Abánades, A. Blanco, A. Burgos, S. Cuesta, P.T. León, J. M. Martínez-Val,
M. Perlado**

Universidad Politecnica de Madrid, 28006 Madrid, Spain

I. Gonçalves, P. Vaz

Instituto Tecnológico e Nuclear, 2686-953 Sacavem, Portugal

Abstract

Some design options for transmutation devices are under consideration, one of them includes a window target cooled by eutectic Lead Bismuth for a gas cooled transmutation core. In this paper we will show the neutronic calculations that we have performed to obtain the heat deposition in the target material, the neutron flux produced in the target and the radiation damage in the structural material for the window target of the gas cooled option of the PDS-XADS project.

For the 6 mA – 600 MeV proton beam, the energy deposition in the window structure reaches more than 800 W/cm³ and more than 2/3 of the total energy of the beam is deposited in the target as heat. The rest of the energy is carried away by the 13 neutrons per proton that enter the surrounding core. The radiation damage and gas production is a very limiting aspect in the design reaching 29 dpa/mA and maximum Hydrogen production of 3000 appm/mA for a full year operation.

Introduction

The PDS-XADS envisages a subcritical experimental reactor driven by a lead-bismuth spallation neutron source. This neutron source is located into the core as a separate device. This neutron source should be capable of delivering a large neutron flux in order to keep the neutron population and, therefore, the nuclear power produced depending on the subcriticality level.

Several calculations have been performed using MCNPX [1], a code that is able to simulate high energy interactions resulting from proton induced spallation reactions and the medium/low energy transport phenomena involving the reactor neutronics in the core.

The study was performed in two steps. In the first step it was considered only the spallation target isolated from the core and it was obtained the heat deposition due to protons and neutrons in the beam window and the region in the target around that window. In the second step, the heat deposition in the target was evaluated taking into account the full reactor geometry, and therefore the contribution due to the neutron flux incoming the target from the reactor in design conditions.

The analysis of both calculations gives very useful information about the effect of the reactor core neutronics in the neutron source (resulting of the subtraction of the two heat deposition data sets) or the behaviour of the spallation source during testing and decommissioning (first tests on site with unloaded core). This separate analysis might give some key ideas about the effect of the core neutronics in the target operation into the core, for instance, to see the increase in power deposition in the target (that should be cooled by the target liquid metal). The power deposition could disturb the heat deposition patterns into the target in such a way that cooling phenomena could be affected. This effect will be discussed throughout this document.

In addition, results of the radiation damage calculations for the window target will be shown and analysed. Radiation damage is foreseen to be one of the most limiting aspects in the overall design of the beam window of an ADS. The beam window, that keeps the beam tube void in the beam transport to the inner part of the subcritical core, is one of the most critical component in the ADS, as it is exposed to a high radiation level, at relative high temperatures, producing high mechanical stresses, and corrosion by liquid metal on the outer side. This radiation damage study will show an estimation of the displacement per atom (dpa) in the beam window and other structural materials on the target, as well as the gas production (Helium and Hydrogen) for the prevention of swelling phenomena in the window structure.

Methodology

The simulation has as starting point the beam characteristics provided by the accelerator requirements in the PDS-XADS project. The beam profile is an elliptical distribution of the form:

$$f(x) = \frac{1}{0.6667} \cdot \frac{I}{\pi \cdot r_0^2} \cdot \left(1 - \frac{r^2}{r_0^2}\right)^{0.5}$$

where I is the proton beam intensity (mA) and r_0 is the beam spot radius (8 cm). The proton kinetic energy is 600 MeV. The maximum beam intensity has been fixed to 6 mA. Nevertheless, the characteristics of the Monte Carlo calculation makes the neutronics and heat deposition results normalised per beam intensity. Therefore, the results could be easily scaled to the operating beam intensity, that it is foreseen from 2.9 to 5.7 along the cycle of the gas cooled accelerator driven system.

The heat deposition has been estimating using the MCNPX 2.5 code, based in Monte Carlo techniques. The input of that code is the beam profile and the reactor description, and we obtain the heat deposition in the regions defined by the user. The heat deposition is estimated in the whole structural material and by a large matrix containing the data in function of appropriate coordinates to couple with the thermal-hydraulic calculations. For that reason the grid used to generate the heat deposition data was quite fine, therefore, as we are handling with a Monte Carlo code, a large computing effort was needed to obtain results with reasonable statistical errors per cell.

The MCNPX code includes high energy physics, that are needed to simulate the spallation reactions resulting from the 600 MeV protons that are delivered by the accelerator through the beam pipe into the center of the target assembly and the core.

The geometry is fully described in the run, including the reactor geometry with one enrichment zone fuel bars and bundles, as well as the reflector and shielding surrounding the core. For heat generation analysis, the first step on the calculation has described the target itself out of the reactor core. In the second step, we repeat the analysis with the fully reactor geometry. The target assembly geometry model is shown in Figure 1.

From the computational point of view, both calculation differ basically on the amount of computer effort required for a reasonable amount of statistics, as the most complex is the geometry, the most demanding is the computing effort to obtain a good statistical estimation. The analysis has been made taking into account the heat deposition due to neutron and proton interaction in the target. The sum of these two contributions results in the total heat deposition that should be the input for the thermal-hydraulic calculation. The heat deposition has been estimated with different meshes, in order to minimize statistical errors in a reasonable computing time. The meshes consists of rectangular annulus centered in the beam axis according to the cylindrical geometry of the whole target.

The radiation damage is estimated from the neutron and particle flux calculated in the structural materials. The proton damage is estimated from the proton flux convoluted with a damage cross section for protons with steel. The neutron damage has been estimated in a similar way convoluting the neutron flux with a damage cross section obtained by the HEATR module of the NJOY data base processing code, in this case for Iron and JENDL3.2. The threshold energy of 2x40 eV to produce an atom displacement and the effective energy coefficient of 0,8 has been taken into account in both cases.

The gas production has been estimated with Monte Carlo methods by the MCNPX code, calculating the effective reaction rate for H, He3 and He4 production and normalising the data with the molecular density and beam characteristics to obtain the amount of appm in each case.

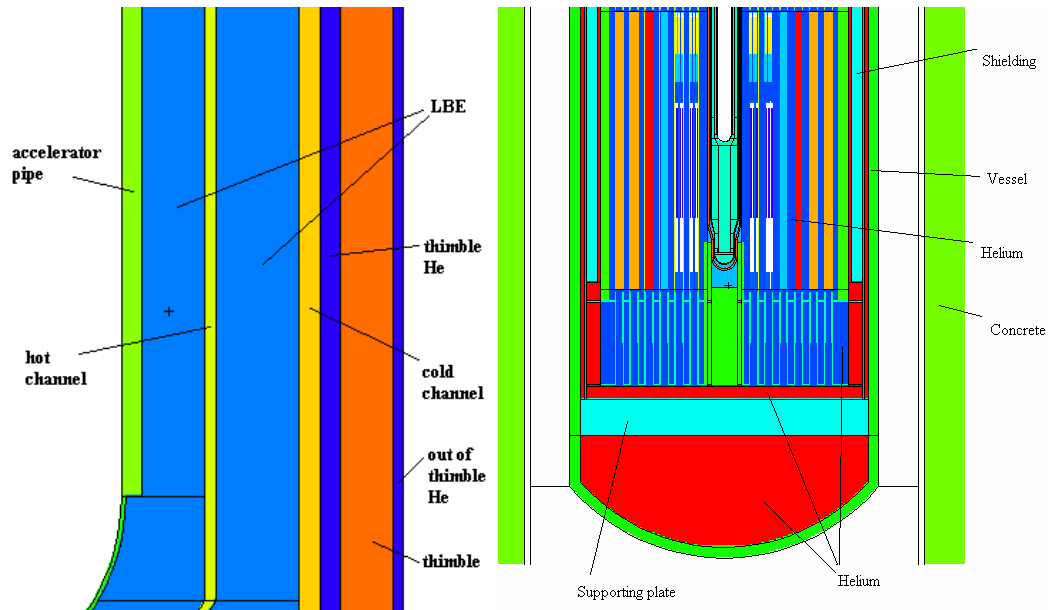


Figure 1: Modelization of the target and subcritical device assembly geometry.

Heat deposition by proton interaction.

The heat deposition by protons are the most important as they are the most energetic particles in the target, that deposit their energy by ionization losses or nuclear interaction processes. The whole energy contained in the impinging protons is absorbed in the target.

This energy deposition is not affected by the operation of the core, as this particles are not produced by nuclear interaction in the core.

In Figure 2, we show the distribution of the energy deposited in the target by the proton interaction. The parabolic distribution of the beam profile determines the heat distribution into the target. The depth of the spallation region also depends on the beam energy trough its particle range in the target material (eutectic Pb/Bi). The range of 600 MeV protons into the target material is about 30 cm. We can see the Bragg peak of the incident protons that are not terminated with spallation reactions.

The energy contribution from proton interaction is the same in both configuration under study, as the protons are only coming from the beam tube. We have simulated the proton interaction in the two configurations, out-of-the-core and into-the-core target, giving the same results, as compared in Table 1. In Figure 7 (note that we use the same scale), we show the total energy deposition in the target, therefore we can see how the proton contribution is practically the 100 % of the total heat deposition in the target. This deposition is not dependant on the integration of the target in the core, what implies that the local analysis performed for the thermal-mechanical-structural design of the window target could be done neglecting the core influence for a first estimation.

In Figure 3 we show the energy deposited in the beam window in function of the angle referred to the beam axis. In this case 180° means the negative z coordinate axis, in the direction of the proton

beam. The 90° angle means the plane perpendicular to the beam axis. The proton heat deposition profile depends on the proton beam distribution and it is produced by ionization losses in the window material (basically stainless steel). This heat is removed by the eutectic Pb/Bi that acts as coolant of the window.

There is a negligible energy deposition by proton interaction in the other structural materials ($< 1 \text{ W/cm}^3$), as could be seen in following paragraphs on the present document.

Heat deposition by neutron interaction.

The heat deposition by neutrons has been estimated in the two scenarios that have been mentioned: target out the core and into the core. The window target calculation out of the core shows the heat generation by neutrons produced by spallation reactions from proton collision with Lead/Bismuth nuclei. These neutrons are basically high energy neutrons that can induce reactions as (n,xn) and bismuth fission.

Figure 4 show the energy deposition by neutrons in the two reference configurations. Note the change in scale of the energy deposition. In Figure 5, the comparison analysis between the energy deposited by neutrons in the two configurations is shown: the target into the core and the target out of the core. It is observed as the amount of energy desposited in the target by neutrons is more than two times higher in the case of the target into the core, as it was expected from external neutrons addition. The neutrons entering the target from the subcritical assembly are less energetic, and therefore, has more probability to induce reactions on the target materials. As it can be seen in the Figure 6, the difference is higher, in the region away from the spallation process location (more than a factor 8 in some cases).

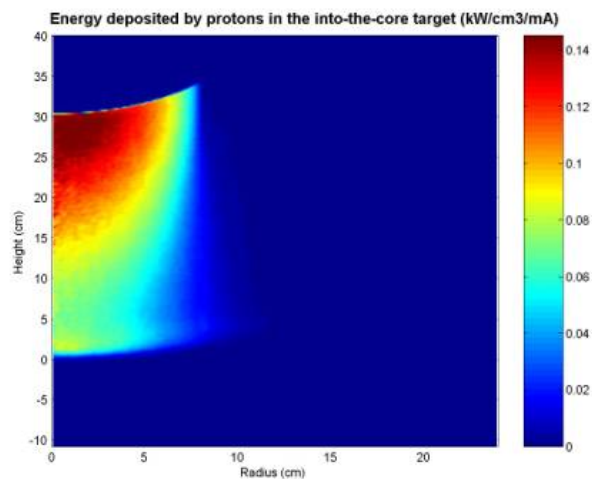


Figure 2: Energy deposited by protons in the target region.

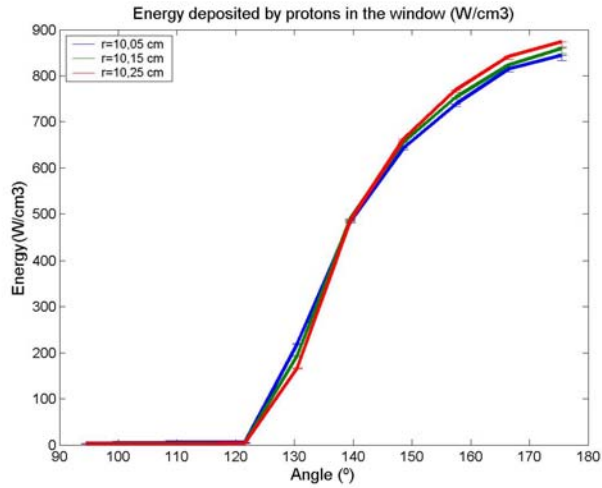


Figure 3: Energy deposition by protons in the beam window.

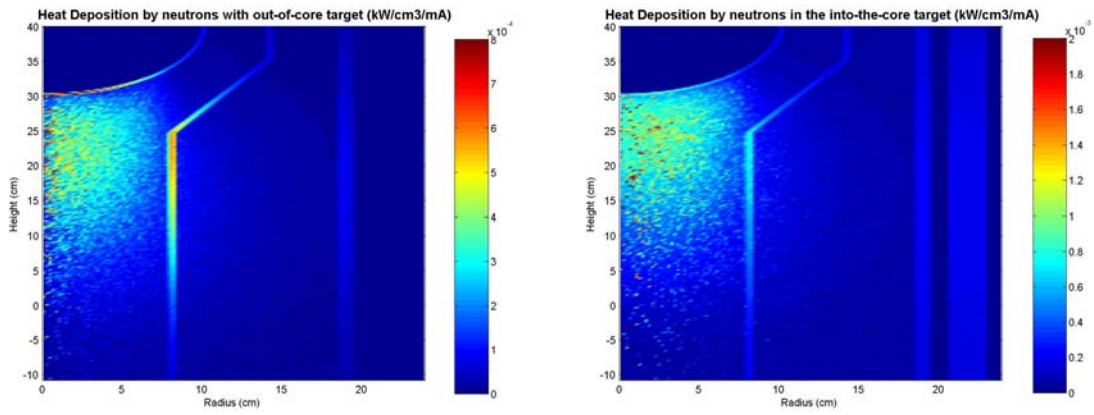


Figure 4: Energy deposited in the target region out-of-the-core and into-the-core configuration

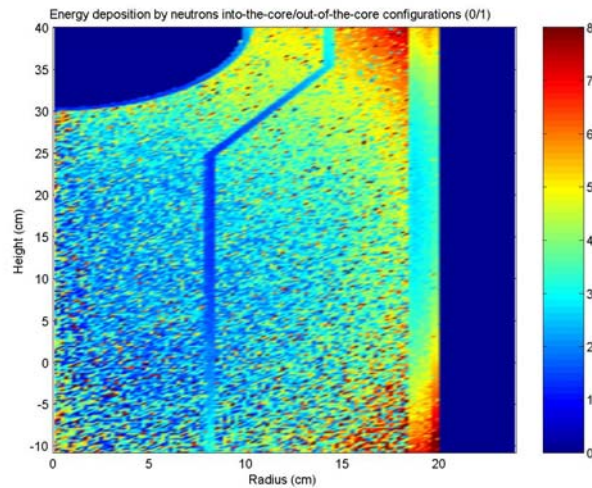


Figure 5: Neutron energy deposition ratio between both configurations.

The region where the neutrons are produced by spallation has high neutron fluxes that results in a more similar heat deposited by neutron interaction. On the contrary, in the target regions near the

core, and less influenced by the neutrons originated by spallation, the effect of the surrounding core is a higher energy deposition by the neutrons entering the target. This is particularly important in the thimble and cold tube materials. Note that the ratio between the energy deposited by protons in the thimble and cold tube has an almost concentric distribution centered in the spallation region.

The energy deposited by neutrons in the beam window has a maximum in the lower pole of the hemispherical structure, just in front of the spallation region. The energy deposition in the structural material of the beam window decrease to energy density levels comparable to that ones obtained for the cold channel (main shell) and thimble (about 1 W/cm^3).

The data about heat deposition by neutrons in the main shell and window suggests that there will be a certain background neutron flux after the insertion of the target in the core that produced a heat deposition in the steel structures of the order de 1 W/cm^3 , for a 6 mA beam intensity.

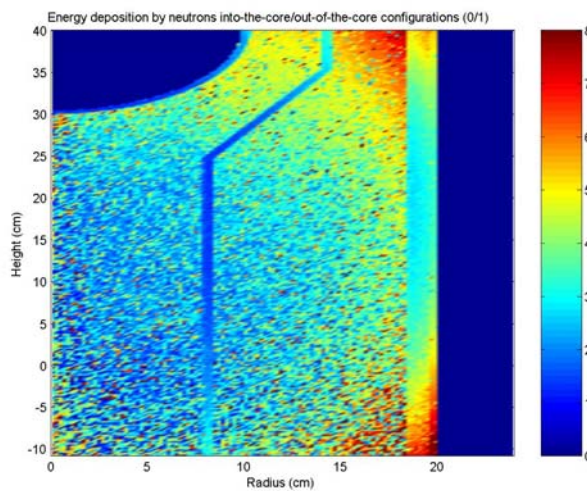


Figure 6: Neutron energy deposition ratio between both configurations.

Total heat deposition.

The total heat deposition in the target takes into account the contributions from proton and neutron interaction within the target material. We can see how the power deposited by protons is the same in both configurations, as expected. Neutron contribution to the energy deposition is higher for the target integrated in the core, as it receives neutrons coming from the core. This effect is particularly important in the regions near the core.

In the Table 1, we show the energy deposition by neutrons and protons in the whole target structure for a beam intensity of 6 mA. The values for the protons and the neutrons "out-of-the-core" can easily be scaled to get the energy deposition at any other beam intensity as this parameter is a linear normalization factor. The values for the core neutrons are almost independent of the beam. They depend on the criticality level of the core. We see how the energy deposited in the core by neutron interactions when the target is in the core is a factor 3 higher in the target region (filled with eutectic Lead/Bismuth). This factor is foreseen to be even larger in the case of the structural materials closer to the core and more distanced from the spallation neutron generation region. This is the case of the Thimble and the cold channel (main shell).

Power (kW)	Protons		Neutrons	
	Into-the-core	Out-of-the-core	Into-the-core	Out-of-the-core
Window	37,91	37,66	0,424	0,3
Target	2322,7	2311,8	48,7	14,95
Cold channel (main shell)	4,38	-	16,2	-
Hot channel (flow skirt)	57	-	6,15	-
Thimble	9,8	-	43,4	-
Total	2431,79	2349,46	114,87	15,24

Table 1: Energy deposition in the target assembly (kW).

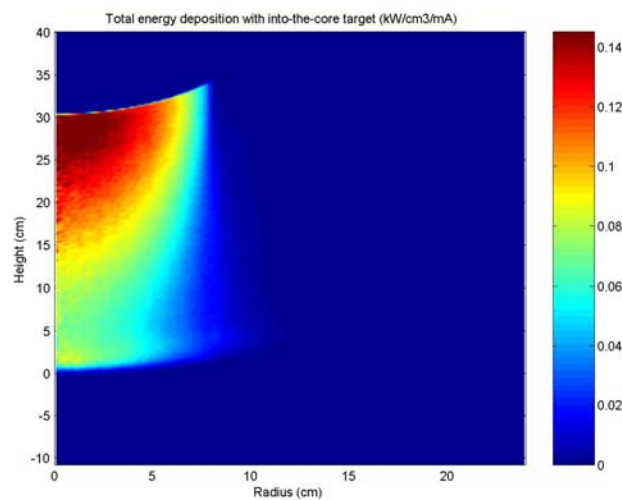


Figure 7: Energy deposition in the target.

Radiation damage calculation

The radiation damage calculation has been estimated for the two types of particles: protons and neutrons. Some other particles, as pions, has been neglected due to the low beam energy. In this section, results of dpa by protons and neutrons will be shown.

In Figure 8 the dpa calculation in the window from protons and neutrons is presented. As it was expected, the maximum damage is produced in the pole of the hemispheric window. In the case of protons, the beam distribution is maximal in the spot centre, producing a more intense protonic damage. For neutrons, the pole of the window is the nearest point in the structure to the neutron generation source, and it is, therefore, the most exposed to the neutron flux. We obtained in this point an estimated amount of 29,8 dpa/year/mA only by neutrons, what constitutes the highest value of all the target components.

Proton damage is focused in the region close to the window and the spallation region. Nevertheless, the proton contribution to this structure is almost negligible (<5% at maximum in a very small location) and the neutron contribution to the material damage is important in a more extent portion of the material. The flow skirt is exposed to an intense neutron flux, comparable to the window.

The proton damage in the cold channel (main shell) and reactor thimble is more acceptable and the maximum neutron damage is of the order of 6 dpa/mA/year. A summary of the maximum neutron flux per proton beam and its maximum radiation damage by protons and neutrons is shown in Table 2.

Table 2: Maximum radiation damage due to protons and neutrons in the window target if the gas cooled PDS-XADS.

	Tot. Proton Flux (h/cm²/ip)	Dpa/year/mA	Tot. Neutron Flux (n/cm²/ip)	Dpa/year/mA
Window struct.	0,00943	5,56745	0,06856	29,86103
Hot channel	6,73707E-4	0,39773	0,06457	16,52564
Cold channel	2,72001E-6	0,00137	0,04427	6,43206
Thimble	1,91887E-6	0,00113	0,04172	6,01715

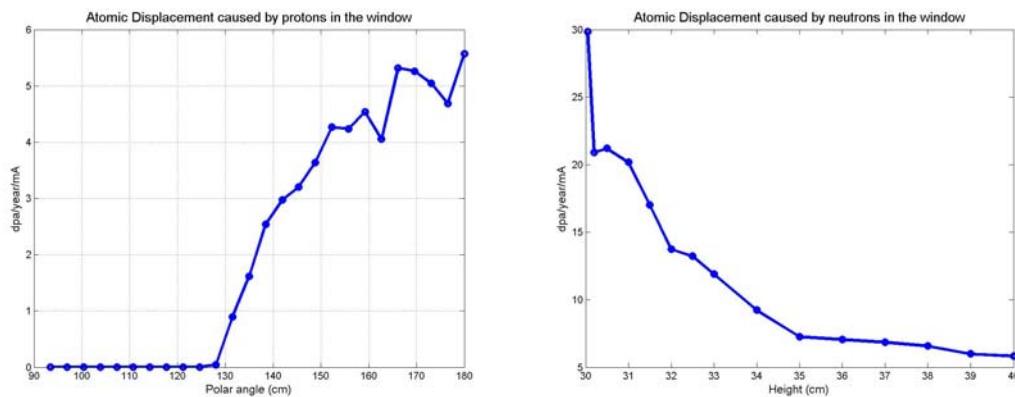


Figure 8: Radiation damage (dpa) in the window by protons and neutrons.

Gas production

The gas production has been obtained with the evaluation of gas formation reactions (n,H), (n,He4) and (n,He3) by means of Monte Carlo simulation with the MCNPX code. The result is the convolution of this reaction cross section with the neutron flux at each points.

In the Table 3, the average gas production is shown at each structural material. In figures, we see the detailed gas production in function of the location. Note that there is points in which gas production is a factor 5 higher than the average data, as a consequence of the higher neutron flux.

The average results in the structural materials (Table 3) shows how the more intense gas production is in the window structure, as expected. Nevertheless these are average results in the whole structure, that may be discussed taken into account the gas production in the positions near to the spallation target.

Table 3: Average gas production in the structure of the target window

	H (appm/y/mA)	He3 (appm/y/mA)	He4 (appm/y/mA)
Window struct.	614,18	0,0051	203,63
Hot channel	251,7	0,003	85,45
Cold channel	19,8	6,7 e-5	4,99
Thimble	21,3	5 e-5	5,35

Figure 9 shows how the pole of the hemispheric window has the highest Hydrogen production (3000 appm/year/mA) as a consequence of the more energetic and intense neutron flux in that point, as with the radiation damage calculation. The maximum Helium production is almost 1200 appm/year/mA., also in the same critical point.

In the hot channel, the peak in the gas production is located in the region near the spallation region. The gas production is also high in those points, although is almost a factor 3 less than in the target window. As in the case of the radiation damage calculation, a special care must also be taken for the material selection of the hot channel (flow skirt).

Table 3: Maximum gas production in the structure of the target window

	H (appm/y/mA)	He4 (appm/y/mA)
Window struct.	3024	1133
Hot channel	1217	443
Cold channel	254	75
Thimble	233	65

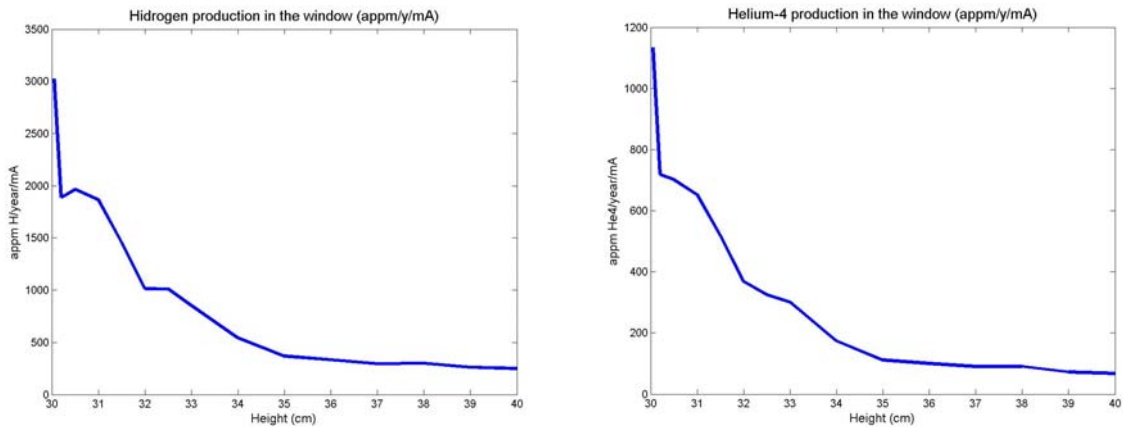


Figure 9: Hydrogen and Helium production in the window.

The gas production in the reactor thimble and cold channel is a factor 10 lower than in the window and it is basically produced by the neutrons travelling out of the target and entering the core. The gas production will be comparable (a little bit higher) to the production in the core. Table 3 shows the maximum gas production at each structure of the target.

Conclusions

Results obtained for a Monte Carlo heat deposition simulation of the target assembly for the PDS-XADS subcritical device have been presented and analyzed. We have made this simulation in two steps. The first one includes only the target assembly and the proton beam, in order to determine the heat deposited by the phenomena derived from spallation processes in the target. The second step envisages the target assembly integrated in the nuclear core of the PDS-XADS, and therefore, including the effect of the operation in nominal conditions.

The global effect on the energy deposition by neutrons in the target assembly as a result of the operation of the target into the core is almost negligible in comparison with the energy deposition produced by protons. The main effect of the operation is the increase in the energy deposited by neutrons, but this component is less than 3 % of the total energy deposition in the core, what is comparable to the error (not only statistical, but also concerning evaluation of the data used for the computational analysis). In fact, the neutrons coming from the reactor can be considered in the main target region as a noise or light perturbation that is added to the system as systematic error of the order of 3%. This assumption is especially convenient to validate local thermalhydraulic calculations in the spallation region, where the location of the target into the core introduces a negligible effect in comparison to the isolated target calculation.

In the thimble and cold channel (main shell), the energy deposited by neutron interaction is the main contributor to the energy deposition, although it is 2 orders of magnitude lower than in the central region of the target.

It is worth pointing out that the total beam energy deposited in the target as heat, is about 2400 kW in the nominal case (6 mA). This is about 2/3 of the total energy of the beam (which has a power of 3600 kW). The rest of the energy is carried away by particles not totally interacting with the target. They are mainly the neutrons feeding the core. 13 neutrons per proton are produced in the target, totalizing 193 MeV (from 600 MeV protons).

The radiation damage and the gas production in the structural material of the beam target seems to be one of the most challenging aspects in the development of a practical high neutron flux generation target for the PDS-XADS. The neutronic conditions derived from the proton energy and the neutron generation region in the liquid lead-bismuth implies that certain parts in the target window is exposed to a high energetic and intense neutron flux. This flux induces a high radiation damage and gas production, especially in the pole of the hemispheric window and certain locations in the hot channel (flow skirt), near to the spallation neutron generation.

References

[1] John S. Hendricks. " MCNPX, Version 2.5.D ". LA-UR-03-5916. Los Alamos National Laboratory.